6-6-2007

Exact Relativistic Beta Decay Endpoint Spectrum

Joseph Schechter
Syracuse University

S. S. Masood
University of Houston - Clear Lake

Exact relativistic beta decay endpoint spectrum

S. S. Masood,[1,][*] S. Nasri,[2,][†] J. Schechter,[3,][‡]

M. A. Tórtola,[4,][§] J. W. F. Valle,[5,][¶] and C. Weinheimer[6,][**]

[1]Department of Physics, 2700 Bay Area Blvd.,

University of Houston Clear Lake, Houston, TX 77058, USA

[2]Institute for Fundamental Theory, University of Florida, Gainesville, FL, USA

[3]Department of Physics, Syracuse University, Syracuse, NY 13244-1130, USA

[4]Departamento de Física and CFTP, Instituto Superior Técnico

Avenida Rovisco Pais 1, 1049-001 Lisboa, Portugal

[5]AHEP Group, Institut de Física Corpuscular – C.S.I.C./Universitat de València

Edificio Institutos de Paterna, Apartado: 22085, E–46071 Valencia, Spain

[6]Institut für Kernphysik, Westfälische Wilhelms-Universität Münster

Wilhelm-Klemm-Str. 9; D-48149 Münster, Germany

(Dated: February 1, 2008)

Abstract

The exact relativistic form for the beta decay endpoint spectrum is derived and presented in a simple factorized form. We show that our exact formula can be well approximated to yield the endpoint form used in the fit method of the KATRIN collaboration. We also discuss the three neutrino case and how information from neutrino oscillation experiments may be useful in analyzing future beta decay endpoint experiments.

[*]Electronic address: masood@uhcl.edu

[†]Electronic address: snasri@ufl.edu

[‡]Electronic address: schechte@phy.syr.edu

[§]Electronic address: mariam@cftp.ist.utl.pt

[¶]Electronic address: valle@ific.uv.es

[**]Electronic address: weinheimer@uni-muenster.de

I. INTRODUCTION

The discovery of neutrino oscillations [1, 2, 3, 4, 5] probes the neutrino squared mass differences and mixing angles [6], but leaves open the issue of what is the absolute scale of neutrino mass. The latter has important cosmological implications in the cosmic microwave background and large scale structure in the Universe, as already indicated by the sensitivities reached, for example, by the recent WMAP-3 [7], the 2dF Galaxy Redshift Survey [8] and Sloan Digital Sky Survey results [9]. One expects even better sensitivities in the next generation of cosmological observations [10, 11]. Interesting as these may be, there are essentially only two ways to get insight into the absolute scale of neutrino mass in the laboratory: searches for neutrinoless double beta decay [12] and investigations of the beta spectra near their endpoints [13, 14, 15, 16, 17, 18]. For the latter direct search for the neutrino mass a very low beta endpoint is crucial: tritium was used in the most sensitive spectrometer experiments [14, 15] and rhenium in the up-coming cryobolometer experiments [19].

Currently a next generation tritium beta-decay experiment is being prepared, scaling up the size and precision of previous experiments by an order of magnitude, and increasing the intensity of the tritium beta source: the KArlruhe TRItium Neutrino experiment KA-TRIN [13, 16, 17, 18]. Such an improved sensitivity experiment will probe neutrino masses ten times smaller than the current limits and therefore play a crucial role in probing for direct effects of neutrino masses.

Prompted by the prospects that high sensitivities can be achieved in the next generation of high precision neutrino mass searches from tritium beta decay experiments [16, 17] we reexamine the accuracy of the kinematical formulae used in the determination of neutrino masses from the shape of the endpoint spectrum. We also discuss the interplay of neutrino oscillation data and the expectations for the beta decay endpoint counting rates for the different types of neutrino mass spectra.

II. RELATIVISTIC BETA DECAY KINEMATICS

In what follows we label the relativistic momenta and energies involved in tritium beta decay according to

$$^3H(\mathbf{0}, M) \rightarrow\, ^3He^+(\boldsymbol{p'}, E') + e^-(\boldsymbol{p_e}, E_e) + \bar{\nu}_e(\boldsymbol{p_\nu}, E_\nu). \tag{1}$$

The masses of $^3He^+$, e^- and $\bar{\nu}_e$ are denoted by M', m_e and m_ν respectively. In order to see the convenience of an exact relativistic description we mention, as recently noted in Ref. [20] that the well known relativistic formula for the maximum electron energy

$$E_e^{max} = \frac{1}{2M} \left[M^2 + m_e^2 - (m_\nu + M')^2 \right],\tag{2}$$

gives a value about 3.4 eV lower than the approximation $M - M' - m_\nu$ often used. This suggests the desirability of carrying out the full phase space integration using relativistic kinematics.

Start from the standard formula for the decay width at rest,

$$\Gamma = \frac{1}{2^9 \pi^5 M} \int \frac{d^3 p_e d^3 p_\nu d^3 p'}{E_e E_\nu E'} |\mathcal{M}|^2 \delta^4(p_{\text{initial}} - p' - p_e - p_\nu),\tag{3}$$

where $|\mathcal{M}|^2$ denotes the spin-summed, Lorentz invariant "squared" amplitude. To explore the constraint of Lorentz invariance one might a priori consider expanding $|\mathcal{M}|^2$ in terms of invariants constructed from the four-momenta. For example, up to two powers of momenta, the most general form is,

$$|\mathcal{M}|^2 = A - B p_e \cdot p_\nu - C p' \cdot p_{\text{initial}} + ...,\tag{4}$$

where A, B and C are constants. Now it is easy to perform some initial integrations. As usual $\int d^3 p'$ is first done with the momentum delta-function. Then the angle between $\mathbf{p}_e$ and $\mathbf{p}_\nu$ is eliminated using the energy delta function. Three more angular integrals are trivial. As the result one may replace in the ^3H rest frame

$$|\mathcal{M}|^2 \rightarrow A + B(E_e E_\nu - \mathbf{p_e} \cdot \mathbf{p_\nu}) + CM(M - E_e - E_\nu),\tag{5}$$

where

$$\mathbf{p_e} \cdot \mathbf{p_\nu} \equiv \frac{1}{2} \left[M^2 - M'^2 + m_e^2 + m_\nu^2 - 2ME_e + 2E_\nu(E_e - M) \right].\tag{6}$$

Eq. (5) can now be inserted in the resulting usual formula [21]

$$\Gamma = \frac{1}{2^6 \pi^3 M} \int dE_\nu dE_e |\mathcal{M}|^2.\tag{7}$$

Next we find $d\Gamma/dE_e$ by integrating over dE_ν for each E_e. The limits of integration $E_\nu^{min}(E_e)$ and $E_\nu^{max}(E_e)$ can be read from [21]. The most tedious part of the present calculation is finding the factorizations:

$$E_\nu^{max} - E_\nu^{min} = \frac{2Mp_e}{(m_{12})^2} (E_e^{max} - E_e)^{1/2} \left[E_e^{max} - E_e + \frac{2m_\nu M'}{M} \right]^{1/2},\tag{8}$$

$$E_\nu^{max} + E_\nu^{min} = \frac{2M}{(m_{12})^2}(M - E_e)\left[E_e^{max} - E_e + \frac{m_\nu}{M}(M' + m_\nu)\right], \tag{9}$$

wherein:

$$(m_{12})^2 = M^2 - 2ME_e + m_e^2. \tag{10}$$

The importance of the factorization is that it makes the behavior at the endpoint $E_e = E_e^{max}$ transparent. Then we have the exact relativistic result,

$$\frac{d\Gamma}{dE_e} = \frac{1}{(2\pi)^3}\frac{p_e}{4(m_{12})^2}\sqrt{y\left(y + \frac{2m_\nu M'}{M}\right)}[A + CM(M - E_e) +$$

$$+ BM\frac{ME_e - m_e^2}{(m_{12})^2}\left(y + \frac{m_\nu}{M}(M' + m_\nu)\right) - C\frac{M^2}{(m_{12})^2}(M - E_e)\left(y + \frac{m_\nu}{M}(M' + m_\nu)\right)] \tag{11}$$

where $y = E_e^{max} - E_e$.

As it stands, this formula is based only on the kinematical assumption in Eq. (4). It obviously vanishes at the endpoint $y = 0$ as $\sqrt{y}$. Note that all other terms are finite at $y = 0$. The overall factor $\sqrt{y(y + 2m_\nu M'/M)}$ gives the behavior of $\frac{d\Gamma}{dE_e}$ extremely close to $y = 0$ for any choice of A, B and C, but departs from $\frac{d\Gamma}{dE_e}$ away from the endpoint.

Dynamics is traditionally put into the picture [22] by examining the spin sum for a 4-fermion interaction wherein the nuclear matrix element is assumed constant. This is presented as a non- Lorentz invariant term,

$$|\mathcal{M}|^2 = BE_e E_\nu. \tag{12}$$

We will see that this is excellently approximated in our fully relativistic model by,

$$A = C = 0, \quad B \neq 0. \tag{13}$$

A more accurate treatment of the underlying interaction might give rise to small admixtures of non-zero A and C as well as other unwritten coefficients in Eq. (4) above.

The form for the spectrum shape near the endpoint that results from putting $A = C = 0$ in Eq. (11) is

$$\frac{d\Gamma}{dE_e} = \frac{p_e MB}{(2\pi)^3 4(m_{12})^4}(ME_e - m_e^2)\sqrt{y\left(y + \frac{2m_\nu M'}{M}\right)}\left[y + \frac{m_\nu}{M}(M' + m_\nu)\right]. \tag{14}$$

Note that if we had employed the non-relativistic form given in Eq. (12) the net result would be a replacement of an overall factor in Eq. (14) according to,

$$(ME_e - m_e^2) \rightarrow (ME_e - E_e^2). \tag{15}$$

4

The difference of these two factors yields the contribution of the $\mathbf{p_e} \cdot \mathbf{p_\nu}$ term. It is really negligible near the endpoint region since it is proportional to p_e^2 and is suppressed like $p_e^2/(ME_e)$ compared to unity. We have checked that the result of our calculation with just the $E_e E_\nu$ term agrees with the calculation of Ref. [23], though their result looks much more complicated, as they did not present it in the simpler factorized form given here.

Note that only the two rightmost factors vary appreciably near the endpoint of Eq. (14). If we further approximate $M'/M \to 1$ and $\frac{M'+m_\nu}{M} \to 1$ the endpoint shape is well described by

$$\frac{d\Gamma}{dE_e} \quad \alpha \quad (y + m_\nu)\sqrt{y(y + 2m_\nu)}. \tag{16}$$

Now we compare with the formula used in the experimental analysis [15]

$$\frac{d\Gamma}{dE_e} \quad \alpha \quad (E_0 - V_i - E)\sqrt{(E_0 - V_i - E)^2 - m_\nu^2}. \tag{17}$$

This agrees with the above approximation in Eq. (16) if one identifies

$$(E_0 - V_i - E) = y + m_\nu. \tag{18}$$

Note that E is the non-relativistic energy given by $E = E_e - m_e$. Furthermore, $E_0 - V_i$ is identified with our $(M - M' - m_e - \delta E_e^{max})$. δE_e^{max} is defined by,

$$E_e^{max} = M - M' - m_\nu - \delta E_e^{max}, \tag{19}$$

and was shown in [20] to be independent of m_ν to a good approximation. Thus we see that the exact relativistic endpoint structure obtained here may be well approximated by the form used in the experimental analysis.

Often, authors express results in terms of a variable, x, which from our discussion may be seen to be the same as,

$$x = -y - m_\nu = E_e - E_e^{max} - m_\nu. \tag{20}$$

In Fig. 1, $d\Gamma/dE_e$ as computed from the exact formula, Eq. (14) is compared with its approximate analog as a function of x. As can be seen, the differences between the approximate and exact formulae are tiny.

It may be worthwhile to remark that the exact relativistic kinematical expression in Eq. (14) is no more complicated than the approximation one ordinarily uses.
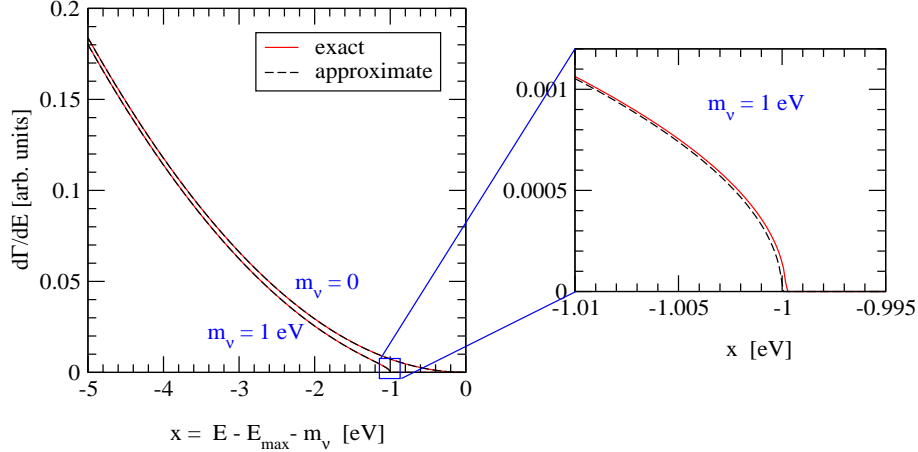
Figure 1: Comparison of approximate and exact formula

III. NUMERICAL SIMULATIONS

We have done Monte Carlo simulations by creating random data sets following the exact relativistic kinematical expression in Eq. (14) for neutrino masses of $m_\nu = 0$ eV and $m_\nu = 1$ eV and fitting them with the standard formula Eq. (17). The simulations were performed for a KATRIN-like experiment [18] considering:

- The ro-vibrational states of the $T_2 \rightarrow (T^3He)^+$ decay [24]

- A signal rate from a KATRIN-like molecular gaseous windowless tritium source with a column density of $5 \cdot 10^{17}$ molecules/cm^2 over an active area of 53 cm^2 and an accepted solid angle of $\Delta\Omega/4\pi = 0.18$

- An expected background rate of 0.01 s^{-1}.

- A response function of a KATRIN-like experiment considering the energy losses within the tritium source and the main spectrometer transmission function with a total width of 0.93 eV.

- 3 years of total data taking covering an energy range of the 25 eV below and 5 eV above the tritium endpoint following an optimized measurement point distribution [18].

Fig. 2 shows the results for the observable m_ν^2 obtained from the fitting of 10000 sets of Monte Carlo data randomized according to the exact relativistic formula Eq. (14) and
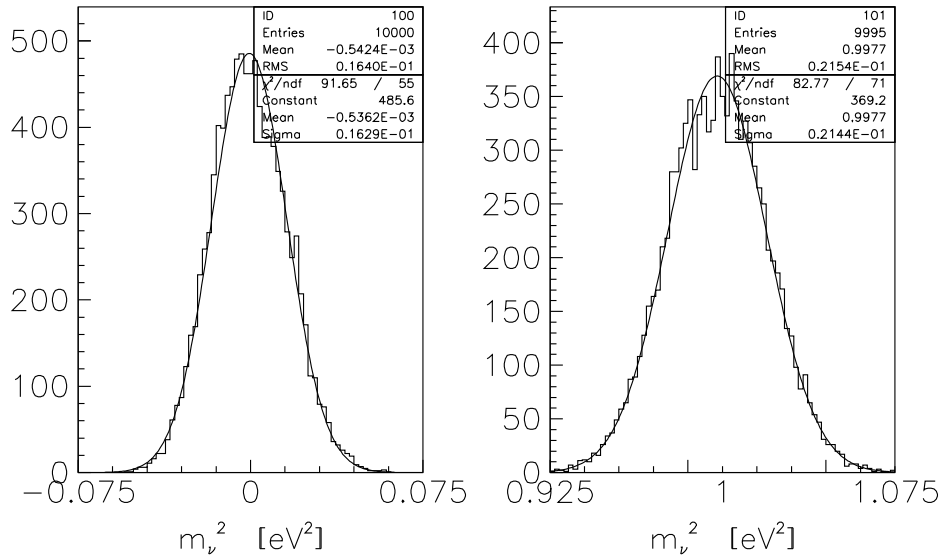
6

Figure 2: Results on the observable m_ν^2 from the fitting of 10000 sets of Monte Carlo data randomized according to the exact relativistic formula Eq. (14) and to a fitting routine based on the standard formula Eq. (17), for neutrino masses of 0 eV (left) and 1 eV (right). The rms values of the Gaussian-like distributions correspond to the expected statistical uncertainty $\Delta m_{\nu,stat}^2$ for a KATRIN-like experiment.

to a fitting routine using the standard formula Eq. (17), assuming neutrino masses of 0 eV (left) and 1 eV (right). The rms values of the Gaussian-like distributions correspond to the expected statistical uncertainty $\Delta m_{\nu,stat}^2$ for a KATRIN-like experiment. Clearly the mean value of the fit results for the neutrino mass squared m_ν^2 does not show any significant deviation from the starting assumption of $m_\nu = 0$ eV or $m_\nu = 1$ eV, respectively. This establishes that the exact relativistic formula Eq. (14) can be well approximated by the standard equation (17) for the precision needed for the next generation tritium experiment KATRIN. This is probably due to the fact that KATRIN is investigating the last 25 eV below of the beta spectrum below its endpoint only, where the recoil corrections are nearly independent on the electron energy.

IV. THREE NEUTRINO CASE

Of course, the most interesting application is to the case of three neutrinos with different masses, m_1, m_2 and m_3. Then there will be a different endpoint energy, E_i^{max} corresponding to each one. The effective endpoint factor in the good approximation of Eq. (16) is the weighted sum,

$$F_{eff}(E_e) = \sum_{i=1}^{3} |K_{1i}|^2 (y_i + m_i)[y_i(y_i + 2m_i)]^{1/2}\theta(y_i), \qquad (21)$$

where $y_i(E_e) = E_i^{max} - E_e$ and the K_{1i} are the elements of the 3x3 lepton mixing matrix [25, 26]. We note that the further good approximation that the quantity δE_e^{max} is independent of the neutrino mass, gives the useful relation

$$y_i - y_j = m_j - m_i. \qquad (22)$$

Now let the unindexed quantity y stand for the y_i with the smallest of the neutrino masses. Using Eq. (22) allows us to write the explicit formula for the case (denoted "normal hierarchy") where m_1 is the lightest of the three neutrino masses as:

$$\begin{aligned} F_{NH}(y) = \; & |K_{11}|^2(y + m_1)[y(y + 2m_1)]^{1/2} \qquad (23) \\ & + |K_{12}|^2(y + m_1)[(y + m_1 - m_2)(y + m_1 + m_2)]^{1/2}\theta(y + m_1 - m_2) \\ & + |K_{13}|^2(y + m_1)[(y + m_1 - m_3)(y + m_1 + m_3)]^{1/2}\theta(y + m_1 - m_3). \end{aligned}$$

In the other case of interest (denoted "inverse hierarchy") we have:

$$\begin{aligned} F_{IH}(y) = \; & |K_{13}|^2(y + m_3)[y(y + 2m_3)]^{1/2} \qquad (24) \\ & + |K_{11}|^2(y + m_3)[(y + m_3 - m_1)(y + m_3 + m_1)]^{1/2}\theta(y + m_3 - m_1) \\ & + |K_{12}|^2(y + m_3)[(y + m_3 - m_2)(y + m_3 + m_2)]^{1/2}\theta(y + m_3 - m_2). \end{aligned}$$

where m_3 is the lightest of the three neutrino masses. From these equations we may easily find the counting rate in the energy range from the appropriate endpoint up to y_{max} as proportional to the integral

$$n_{NH}(y_{max}) = \int_0^{y_{max}} dy \, F_{NH}(y), \qquad (25)$$

or, for the "inverse hierarchy" case, as proportional to,

$$n_{IH}(y_{max}) = \int_0^{y_{max}} dy \, F_{IH}(y). \qquad (26)$$

8

We note that, as stressed in ref. [20], information on neutrino masses and mixings obtained from neutrino oscillation experiments is actually sufficient in principle to predict $n(y_{max})$ as a function of a single parameter (up to a twofold ambiguity). Thus, in principle, suitably comparing the predicted values of $n(y_{max})$ with results from a future endpoint experiment may end up determining three neutrino masses.

To see how this might work out we make an initial estimate using the best fit values [6] of neutrino squared mass differences,

$$A \equiv m_2^2 - m_1^2 = 7.9 \times 10^{-5} eV^2, \tag{27}$$
$$B \equiv |m_3^2 - m_2^2| = 2.6 \times 10^{-3} eV^2,$$

and the weighting coefficients,

$$|K_{11}|^2 = 0.67, \tag{28}$$
$$|K_{12}|^2 = 0.29,$$
$$|K_{13}|^2 = 0.04.$$

Currently $|K_{13}|^2$ is consistent with zero and is only bounded. For definiteness we have taken a value close to the present upper bound. However, we have checked that the effect of putting it to zero is very small. Now, from the two known differences in Eq. (27) we can for each choice of m_3 (considered as our free parameter) find the masses m_1 and m_2, subject to the ambiguity as to whether m_3 is the largest (NH) or the smallest (IH) of the three neutrino masses. Of course we hope that future long baseline neutrino oscillation experiments [27, 28, 29, 30] might eventually determine whether nature prefers the NH or the IH scenario.

Fig. 3 shows typical solutions for the mass set (m_1, m_2) in terms of the free parameter m_3. Very large values of m_3 would fall within the sensitivity of upcoming cosmological tests [10, 11]. In the right panel of Fig. 3 we display the predicted values of $n(y_{max})$ for each possible mass scenario and the choices of (1,10,20) eV for y_{max}. These quantities are proportional to the electron counting rate in the energy interval from the endpoint (for each mass scenario) to y_{max} eV below the endpoint. The different values of y_{max} reflect, of course, different experimental sensitivities. The main point is that, for sufficiently large m_3 values, the counting rate is seen to distinguish the different possible neutrino mass sets from each other. We hope that the present method of relating observed neutrino oscillation
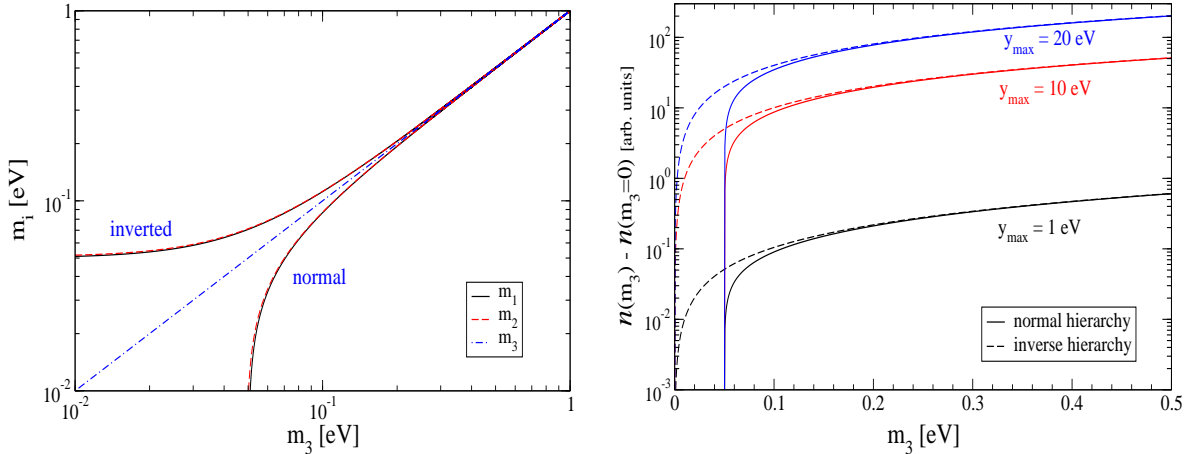
Figure 3: The left panel shows typical solutions for (m_1, m_2) as a function of m_3 for the NH case (solid curves) and the IH case (dashed curves); the middle dot-dashed is given for orientation. The right panel give the predictions for the quantities, $n(y_{max})$, proportional to the event counting rate which includes emitted electrons within, respectively 1 eV, 10 eV and 20 eV from the appropriate endpoint.

parameters to predictions for the beta decay endpoint counting rates may play a useful role in the forthcoming experiments.

V. SUMMARY AND DISCUSSION

We have derived the exact relativistic form for the beta decay endpoint spectrum and presented it in a very simple and useful factorized form. We showed that our exact formula can be well approximated to yield the endpoint form used in the fit method of the KATRIN collaboration. This was explicitly established through a detailed numerical simulation. We have also discussed the three neutrino case and shown how information from neutrino oscillation experiments may be useful in analyzing future beta decay endpoint experiments.

Acknowledgements

[1] Super-Kamiokande collaboration, S. Fukuda *et al.*, Phys. Lett. **B539**, 179 (2002), [hep-ex/0205075].

[2] SNO collaboration, Q. R. Ahmad *et al.*, Phys. Rev. Lett. **89**, 011301 (2002), [nucl-ex/0204008].

[3] KamLAND collaboration, T. Araki *et al.*, Phys. Rev. Lett. **94**, 081801 (2004).

[4] For a review see T. Kajita, New J. Phys. **6**, 194 (2004).

[5] K2K collaboration, M. H. Ahn *et al.*, Phys. Rev. Lett. **90**, 041801 (2003), [hep-ex/0212007].

[6] For an uptaded review see M. Maltoni, T. Schwetz, M. A. Tortola and J. W. F. Valle, New J. Phys. **6**, 122 (2004), hep-ph/0405172 (v5); previous works by other groups are referenced therein.

[7] WMAP collaboration, D. N. Spergel *et al.*, astro-ph/0603449.

[8] M. Colless *et al.*, Mon. Not. R. Astron. Soc **328**, 1039 (2001).

[9] SDSS collaboration, M. Tegmark *et al.*, Phys. Rev. D **69**, 103501 (2004), [astro-ph/0310723].

[10] J. Lesgourgues and S. Pastor, Phys. Rep. **429**, 307 (2006), [astro-ph/0603494].

[11] S. Hannestad, Ann. Rev. Nucl. Part. Sci. **56**, 137 (2006), [hep-ph/0602058].

[12] S. R. Elliott and P. Vogel, Ann. Rev. Nucl. Part. Sci. **52**, 115 (2002), [hep-ph/0202264].

[13] KATRIN collaboration, A. Osipowicz *et al.*, hep-ex/0109033.

[14] V. M. Lobashev, Nucl. Phys. **A719**, 153 (2003).

[15] C. Kraus *et al.*, Eur. Phys. J. **C40**, 447 (2005), [hep-ex/0412056].

[16] G. Drexlin for the KATRIN collaboration, Nucl. Phys. Proc. Suppl. **145**, 263 (2005).

[17] C. Weinheimer, Nucl. Phys. Proc. Suppl. **168**, 5 (2007)

[18] KATRIN collaboration, J. Angrik *et al.*, FZKA-7090 (KATRIN design report 2004).

[19] A. Monfardini *et al.*, Prog. Part. Nucl. Phys. **57**, 68 (2006), [hep-ex/0509038].

[20] S. S. Masood, S. Nasri and J. Schechter, Int. J. Mod. Phys. **A21**, 517 (2006), [hep-ph/0505183].

[21] Particle Data Group, S. Eidelman *et al.*, Phys. Lett. **B592**, 1 (2004).

[22] J. D. Bjorken and S. D. Drell, *Relativistic Quantum Mechanics* (McGraw-Hill, N.Y., 1964).

[23] C.-E. Wu and W. W. Repko, Phys. Rev. **C27**, 1754 (1983).

[24] A. Saenz, S. Jonsell and P. Froelich, Phys. Rev. Lett. **84**, 242 (2000).

[25] J. Schechter and J. W. F. Valle, Phys. Rev. **D22**, 2227 (1980).

[26] Particle Data Group, W. M. Yao *et al.*, J. Phys. **G33**, 1 (2006).

[27] C. Albright *et al.*, hep-ex/0008064, Report to the Fermilab Directorate.

[28] M. Apollonio *et al.*, hep-ph/0210192, CERN Yellow Report on the Neutrino Factory.

[29] P. Huber, M. Lindner and W. Winter, Nucl. Phys. **B645**, 3 (2002), [hep-ph/0204352].

[30] Muon Collider/Neutrino Factory, M. M. Alsharoa *et al.*, Phys. Rev. ST Accel. Beams **6**, 081001 (2003), [hep-ex/0207031].